

Feedback localization of freely diffusing fluorescent particles near the optical shot-noise limit

Andrew J. Berglund, Kevin McHale, and Hideo Mabuchi

Physical Measurement and Control 266-33, California Institute of Technology, Pasadena, California 91125, USA

Received August 7, 2006; revised October 10, 2006; accepted October 12, 2006;
posted October 18, 2006 (Doc. ID 73852); published December 23, 2006

We report near-optimal tracking of freely diffusing fluorescent particles in a quasi-two-dimensional geometry via photon counting and real-time feedback. We present a quantitative statistical model of our feedback network and find excellent agreement with the experiment. We monitor the motion of a single fluorescent particle with a sensitivity of $15 \text{ nm}/\sqrt{\text{Hz}}$ while collecting fewer than 5000 fluorescence photons/s. Fluorescent microspheres (diffusion coefficient $1.3 \mu\text{m}^2/\text{s}$) are tracked with a root-mean-square tracking error of 170 nm, within a factor of 2 of the theoretical limit set by photon counting shot noise. © 2006 Optical Society of America

OCIS codes: 180.2520, 180.5810, 300.2530.

A series of recent experimental and theoretical investigations has begun a new era in closed-loop control of the Brownian motion of individual fluorescent particles.^{1–8} All of these methods use a particle's fluorescence to sense its deviation from a target position and use a feedback network to compensate for the particle's random motion, either by active tracking or trapping. However, a diffusing particle cannot be tracked arbitrarily well at a finite fluorescence count rate, since an overly aggressive feedback controller will feed photon counting noise back into the system.⁸ In this Letter we demonstrate a feedback control system capable of tracking the planar Brownian motion of a freely diffusing particle near this optical shot-noise limit, and we introduce a quantitative model for interpreting experimental statistics.

We use the home-built optical microscope and tracking apparatus described in a previous publication,⁵ with slight modifications. In short, (nominally) 60 and 210 nm diameter fluorescent microspheres diffuse freely in a thin ($\sim 1 \mu\text{m}$) aqueous layer between glass microscope coverslips mounted on a piezoelectric translation stage. We detect the x and y position of a particle by translating our excitation laser in a circular pattern about the optic (z) axis of the microscope. The laser rotates at $\omega_0 = 2\pi \times 8 \text{ kHz}$, a frequency that is large compared with the characteristic diffusion times across our laser focus (45 and 170 ms, respectively, for the 60 and 210 nm diameter microspheres). Our beam waist is $w = 1 \mu\text{m}$, and the rotating laser focus is offset from the optic axis by a distance $r = 0.6 \mu\text{m}$. When a particle diffuses away from the optic axis, its fluorescence is modulated as the laser sweeps past it at frequency ω_0 , and we detect the amplitude and phase of this modulation by using a lock-in amplifier. The resulting cosine and sine quadrature signals provide an error signal proportional to the x and y components of the particle's position. These two error signals are filtered by two analog controllers and sent to a high-voltage amplifier to drive the piezoelectric stage containing the entire bulk sample. In this way, we

translate the bulk sample to compensate for the particle's Brownian motion; the particle is then locked to the optic axis, and the time-dependent position of the sample stage becomes a measure of the particle's diffusion trajectory.

We simultaneously record the position of the sample stage and the arrival times of fluorescence photons during a typical tracking trajectory. A single shot of the experiment is shown in Fig. 1. For the measurements presented here, we used a sample containing roughly equal concentrations of 60 and 210 nm fluorescently labeled microspheres. Because the 210 nm microspheres contain more dye molecules, they appear much brighter than the 60 nm microspheres when illuminated by the same laser intensity. To track both types of particle in a comparable way, we use an electronic servo to adjust the excitation laser power (by modulating the rf power to an acousto-optic modulator) to lock the total photon count rate to 5600 s^{-1} . The photon count rate due to background light was approximately 1000 s^{-1} , inde-

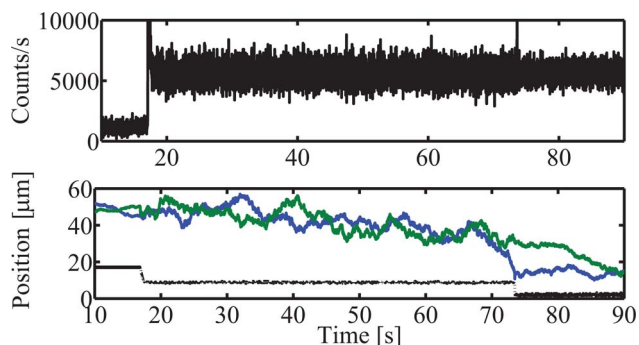


Fig. 1. (Color online) Data from a typical run of the experiment. The upper plot shows the rate of photon detections. In the lower plot, the upper curves are the x and y positions of the sample stage during the same trajectory. The lower curve on the lower plot shows the excitation laser power (in arbitrary units) necessary to lock the number of detected photons to 5600 s^{-1} . The plots show three regions, in which no particle is present (until 17 s), a 60 nm diameter particle is tracked (until 74 s), and a 210 nm diameter particle is tracked (until 90 s).

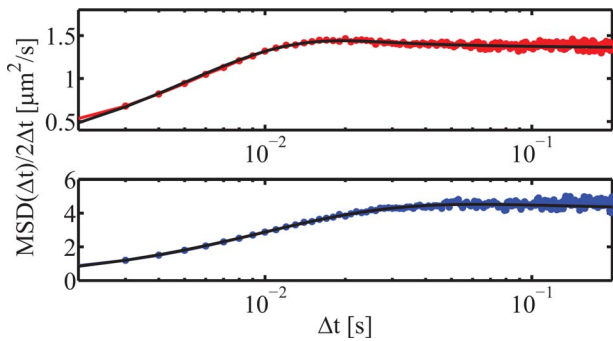


Fig. 2. (Color online) $\text{MSD}(\Delta t)/2\Delta t$ as defined by Eq. (1) for two typical [210 nm diameter (upper) and 60 nm diameter (lower) microspheres] tracking trajectories together with fits to Eq. (5). At long times, the curves approach the particle diffusion coefficient, while the short-time behavior depends on the tracking feedback performance.

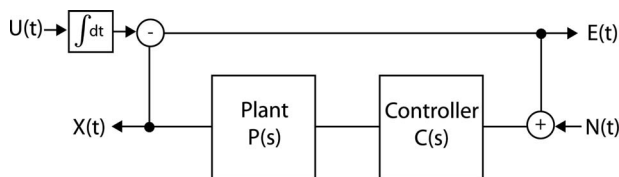


Fig. 3. Block diagram used in the text to represent the particle tracking control system.

pendent of excitation intensity, leaving the rate of fluorescence photon arrivals at 4600 s^{-1} during tracking.

In this Letter we are interested in recovering statistical quantities such as the tracking error and the particle's diffusion coefficient from the position of the sample stage during a tracking trajectory. Let the time-dependent x coordinate of the sample stage position be $X(t)$, and let its mean-square deviation over a time interval Δt be denoted

$$\text{MSD}(\Delta t) = \langle [X(t + \Delta t) - X(t)]^2 \rangle, \quad (1)$$

where $\langle \rangle$ represents an ensemble average. When Δt is much larger than the inverse feedback bandwidth, we expect $\text{MSD}(\Delta t) \approx 2D\Delta t$, the mean-square deviation of a freely diffusing particle with diffusion coefficient D ; however, because of the inevitable roll-off of the feedback response at short times, the sample stage will not move appreciably for small Δt . Thus we expect the mean-square deviation to probe the feedback bandwidth parameters at small Δt and the particle's diffusion coefficient at large Δt . In Fig. 2 we show the measured value of $\text{MSD}(\Delta t)/2\Delta t$, for two different trajectories, together with fits to Eq. (5) based on the model described below.

It was shown in Ref. 8 that for sufficiently good tracking, our experiment may be modeled as a linear control system. We take as our model the linear feedback network shown in Fig. 3, where the tracking controller is represented by the (Laplace space) transfer function $C(s)$ and the piezoelectric stage is represented by $P(s)$. We consider the control system in one dimension only, since the x and y positions of a

Brownian particle are statistically independent. The particle is driven by Brownian motion, and we represent its velocity, $U(t)$, by

$$U(t) = \sqrt{2D} \frac{dW}{dt}, \quad (2)$$

where D is the diffusion coefficient and dW is a stochastic Wiener increment.^{9,10} The time integral of $U(t)$ is the position of the particle at time t . The position of the sample stage is denoted $X(t)$, and the error signal $E(t)$ is the difference between the stage position $X(t)$ and the particle's position. Finally, Gaussian white noise $N(t) = n dW/dt$ with a noise density n is added to the error signal. The noise $N(t)$ must be included in our model to account for photon counting fluctuations, which give rise to a nonzero noise density n for all finite fluorescence intensities.⁸ Of course, any excess technical noise beyond these fundamental limits may also be captured by this parameter. The resulting system is a linear, two-input $[U(t), N(t)]$, two-output $[X(t), E(t)]$ system, which we investigate below.

For our experiment, the controller is a simple integrator with time constant γ_c , and the piezoelectric stage may be sufficiently represented by a first-order low-pass filter with a roll-off frequency $\gamma_p/2\pi$: $C(s) = \gamma_c/s$, $P(s) = 1/(1+s/\gamma_p)$. Because the system is linear, the total output of the system is just the sum of the output resulting from each input considered in isolation. As an example of the response to a single input, consider the sample stage position $X(t)$ when it is driven by the particle's diffusion $U(t)$, with $N(t) = 0$. For our second-order model, we require the velocity of the sample stage $\dot{X}(t) = dX(t)/dt$. Using standard results, we find the following state-space realization of the system¹¹:

$$d\xi(t) = \mathbf{A}\xi(t)dt + U(t)dt, \quad \dot{X}(t) = \mathbf{C}\xi(t), \quad (3)$$

where $\xi(t)$ is a two-component internal state vector and

$$\mathbf{A} = \begin{pmatrix} -\gamma_p & -\gamma_p \\ \gamma_c & 0 \end{pmatrix}, \quad \mathbf{C} = (0 \ \gamma_p). \quad (4)$$

The components of $\xi(t)$ are simply scaled multiples of $X(t)$ and $\dot{X}(t)$. Upon insertion of Eq. (2), Eq. (3) becomes a linear stochastic differential equation, the multivariable Ornstein–Uhlenbeck process.⁹ The resulting solution for $\dot{X}(t)$ is a Gaussian process whose statistics are given by a Fokker–Planck equation, which is exactly solvable.^{9,10} In this way we may calculate the response of any output signal due to any input signal, and by superposition we may construct the full output signal due to all inputs. Of particular interest is the mean-square deviation of the sample stage position. We find

$$\text{MSD}(\Delta t) = 2D\Delta t - \frac{2D\gamma_c}{\gamma_p} \mathbf{C} \mathbf{A}^{-2} \left(\mathbf{I} - \frac{n^2 \mathbf{A}^2}{2D} \right) (\mathbf{I} - e^{\mathbf{A}\Delta t}) \times \begin{pmatrix} 1/\gamma_c & 0 \\ 0 & 1/\gamma_p \end{pmatrix} \mathbf{C}^T. \quad (5)$$

For a stable feedback system ($\mathbf{A} < 0$), we find $\text{MSD}(\Delta t) \approx 2D\Delta t$ for large values of Δt (compared with the feedback time scale). The measurement noise contributes a dimensionless correction matrix $(n^2/2D)\mathbf{A}^2$, which may be used to assess the influence of measurement noise on the system. For the 2×2 system considered here, the matrix exponentials in Eq. (5) may be calculated explicitly; however, the resulting expression is rather complicated and provides little additional insight.

We may extract the particle's localization from the measured motion of the sample stage. We define this localization (along one axis only) to be $L = \sqrt{\langle E(t)^2 \rangle}$, which is the standard deviation of the particle's distance from the sample stage position, i.e., the tracking error. For our system,

$$L = \sqrt{D \left(\frac{1}{\gamma_c} + \frac{1}{\gamma_p} \right) + \frac{n^2 \gamma_c}{2}}. \quad (6)$$

We establish the parameters n , γ_c , γ_p , and D by fitting the curves in Fig. 2 to Eq. (5). We then calculate each particle's localization by using Eq. (6). The resulting values of L are plotted versus the measured diffusion coefficient D in Fig. 4. To confirm the validity of this fitting technique for estimating L , we generated Monte Carlo simulations of the second-order control system driven by diffusion and measurement noise, using typical values of the parameters n , γ_c , γ_p , and D . We then estimated L and D for the resulting data. These results are shown in gray in Fig. 4.

The dashed curves in Fig. 4 show the shot-noise localization limit derived in Ref. 8 for our experimen-

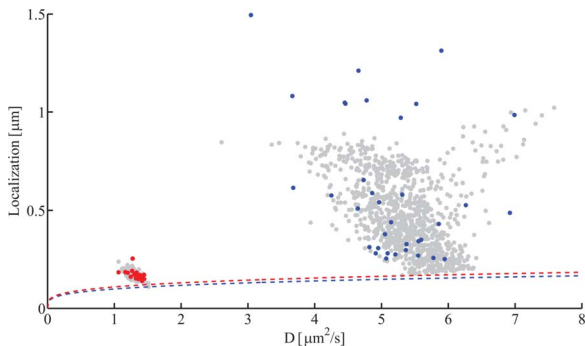


Fig. 4. (Color online) Measured localization L versus D for 62 individual tracking trajectories (dark dots). The lighter dots are the results of simulations described in the text. The dashed curves are the localization limit based on optical shot noise. Typical fit parameters for the 210 nm beads (red online, dark dots clustered in the lower left corner of the plot) are $D = 1.3 \mu\text{m}^2/\text{s}$, $n = 15 \text{ nm}/\sqrt{\text{Hz}}$, $\gamma_c = 111 \text{ Hz}$, $\gamma_p = 343 \text{ Hz}$. The fitted value of γ_c is commensurate with the bandwidth of the analog integrator used for tracking control, while γ_p serves primarily to represent the phase delay of our piezoelectric stage at high frequencies ($\geq 100 \text{ Hz}$).

tally determined values of the beam waist w , rotation radius r , and fluorescence count rate for a particle located at the maximum laser intensity (approximately 15.1 kHz and 9.8 kHz for the 60 and 210 nm particles, respectively). For the 210 nm diameter beads, the mean inferred localization is 170 nm, and the shot-noise limited value is 117 nm. The noise density n for these beads is found to be $15 \text{ nm}/\sqrt{\text{Hz}}$, while the shot-noise limited value is $9.4 \text{ nm}/\sqrt{\text{Hz}}$. The 60 nm beads are more poorly localized, owing to their faster diffusion, but the large spread in the inferred values of L for these particles arises from noise in the fitting procedure, not from a true spread in the underlying tracking error. This claim is supported by the large spread in the localization values inferred from the Monte Carlo simulations, whose underlying localizations were tightly clustered near 300 nm. (A more detailed data analysis including fluorescence fluctuations shows a mean localization of 340 nm for the 60 nm particles, but these results are beyond the scope of this analysis.) Furthermore, the observed values of L for the 60 nm particles stray even beyond the simulations; however, the linear control-system analysis assumes the particles to be well localized relative to r and w ,⁸ and this assumption is not particularly valid for the 60 nm beads. While it is difficult to analyze the statistics of this nonlinear tracking, it is a feature of our experiment that the feedback network is robust enough to track in this regime.

K. McHale acknowledges support from an NDSEG fellowship. This work was supported by NSF grant CCF-0323542 and by the Institute for Collaborative Biotechnologies through grant DAAD19-03-D-0004 from the Army Research Office. Any opinions, findings, and conclusions or recommendations expressed in this material are those of the authors, and do not necessarily reflect the views of either funding agency. A. Berglund's e-mail address is berglund@caltch.edu.

References

1. T. Ha, D. S. Chemla, T. Enderle, and S. Weiss, *Appl. Phys. Lett.* **70**, 782 (1997).
2. J. Enderlein, *Appl. Phys. B* **71**, 773 (2000).
3. A. J. Berglund and H. Mabuchi, *Appl. Phys. B* **78**, 653 (2004).
4. V. Levi, Q. Ruan, and E. Gratton, *Biophys. J.* **88**, 2919 (2005).
5. A. J. Berglund and H. Mabuchi, *Opt. Express* **13**, 8069 (2005).
6. S. B. Andersson, *Appl. Phys. B* **80**, 809 (2005).
7. A. E. Cohen and W. E. Moerner, *Proc. Natl. Acad. Sci. U.S.A.* **103**, 4362 (2006).
8. A. J. Berglund and H. Mabuchi, *Appl. Phys. B* **83**, 127 (2006).
9. C. W. Gardiner, *Handbook of Stochastic Methods for Physics, Chemistry and the Natural Sciences*, 2nd ed. (Springer-Verlag, 1985).
10. N. G. Van Kampen, *Stochastic Processes in Physics and Chemistry* (Elsevier Science, 2001).
11. O. L. R. Jacobs, *Introduction to Control Theory*, 2nd ed. (Oxford U. Press, 1996).